

## INVESTIGATION ON THE INFLUENCE OF INLET DISTRIBUTION ON MOLTEN-SALT THERMOCLINE STORAGE

Letian Wang, Zhen Yang, Yuanyuan Duan

Key Laboratory for Thermal Science and Power Engineering of Ministry of Education  
 Department of Thermal Engineering, Tsinghua University  
 Beijing 100084 China

### ABSTRACT

Thermocline storage system performance plays an essential role in the Concentrated Solar Power (CSP) plants. A molten-salt with filler material based dual-media storage has been recognized as a prominent storage system. The paper has focused on the thermal effects of inlet velocity non-uniformity in dual-media storage in. The radial non-uniformity was studied with setting different percentage of non-flow inlet area. The synthetic effects of plant capacity and non-uniformity are also investigated with a comparison of 200  $MW_e$  and 50  $MW_e$ . Regardless of the power capacity, the radial velocity non-uniformity effects to the overall outflow thermal performance can be neglect. No salient influence for outflow temperature history, and only a small deviation 0.8%, of mass flow rate and flow time has been found. The plant capacity makes no significant change to the results. Thus the effects of non-uniformed inlet velocity have no important impact on dual-media thermocline storage design.

### NOMENCLATURE

f	Storage factor -
R	Rankine efficiency -
q	(200-450°C) equivalent heat capacity of HITEC [J/kg]
$\rho_H$	the density of hot MS[kg/m <sup>3</sup> ]
$\rho_L$	the density of cold MS[kg/m <sup>3</sup> ]
Cp	specific heat[J/kg-K]
d	diameter of thermocline tank[m]
ds	diameter of filler particles[ m]
F	inertial coefficient, $F = \frac{1.75}{\sqrt{150e^3}}$
g	gravity[m/s <sup>2</sup> ]
h	height of thermocline[m]
h'	height of distributor region,[m]
hi	interstitial heat transfer coefficient[W/m <sup>3</sup> -K]
hconv	wall heat transfer coefficient[W/m <sup>2</sup> -K]
K	permeability, $K = \frac{d_p^2 e^3}{175(1-e)^2}$ [ m <sup>2</sup> ]
k	thermal conductivity[ W/m-K]
p	pressure[Pa]

T	temperature[K]
t	time[ s]
<b>u</b>	velocity vector[ m/s]
um	mean velocity magnitude at inlet to fillerbed [m/s]
umag	velocity magnitude [m/s]

### Greek

$\varepsilon$	porosity, -
$\eta$	efficiency, -
$\Theta$	non-dimensional temperature, -
$\mu$	viscosity[Pa-s]
$\nu$	kinematic viscosity[m <sup>2</sup> /s]
$\rho$	density[ kg/m <sup>3</sup> ]

### Subscript

L	at the inlet low temperature
H	at the outlet high temperature
l	molten salt phase
s	solid filler phase

### INTRODUCTION

Thermal energy storage (TES) has been increasingly wide used in the storage system in Concentrated Solar Power (CSP) plants[1]; a molten-salt thermocline with filler material of quartzite rock has been recognized as a prominent solution for the thermocline with a higher energy efficiency and lower cost.[2]

In order to have a better understanding of the storage capacity and energy performance in a thermocline tank with filler material, the flow and heat transfer phenomena should be further studied and illustrated. An integrated parametric and schematic investigation on the discharging process with a uniformed inlet assumption provides some instructive guidelines for the industrial [3]. Yet, almost all of the research on the molten salt storage assumes the uniform inlet velocity condition.[4] The uniformed inlet assumption reduces complexity of previous research to focus on the influence of inlet temperature, mean velocity and so on. However, due to diffuser's configuration, usually manifolds, the inlet is

impossible to have a uniformed velocity; the non-uniformed velocity may synthesize with other conditions and eventually cast strong influence on the storage's thermal performance.

In traditional thermocline applied water storage system, the configurations, though mainly as radial disks and octagonal concentric tubes, are still diversified[5]. And due to the unknowns of the distribution influence, no existing standard was applied in the design and maintain of the filler-based distribution system. Therefore, a deeper investigation can help engineers with design instruments for distribution system.

According to the cylinder configuration of the tank, there are there geometrical factors in the velocity distribution variation. First is in one end of the tank, the velocity varies radially and azimuthally. Secondly, velocity distribution in different end may play different role due to the temperature difference. Take discharge process as basic model, the hot end will be studied as benchmark and we first studied the radial distribution of velocity, therefore the dimension of the model will be reduced to 2D. Afterwards, azimuthal effects will be checked at last with 3D model. As for end factor, the distribution in hot end and cold end will be separately studied. To put the insight into practical guideline for the industry, other factors like power capacity and rock diameter have also been studied to determine the maximum effect of velocity distribution. The outflow temperature history and thermocline stratification contour here are considered thermal performance of the storage tank.

## NUMERICAL MODEL

### Problem description

The schematic illustration of a TES thermoclinr tank is listed in the **Fig.1**. The model is aimed for the discharge cycle where the cold molten-salt (MS) flow from the bottom into the tank and drive the hot MS flow out for Rankine cycle. The wall condition are set adiabatic.

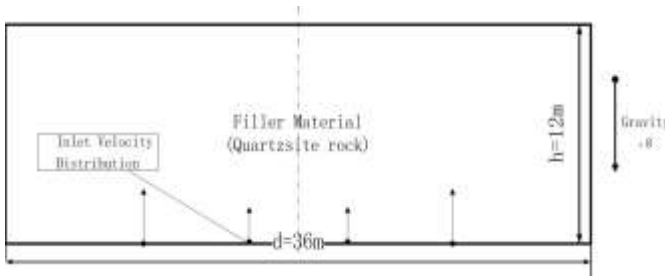


Figure 1 Schematic illustration of tank model

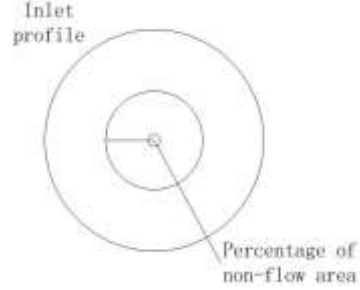


Figure 2 Inlet velocity profile

The tank has a inner diameter of  $d$  and height of  $h$ , and is full of filler quartzite filler. To fully emulate the actual heat capacity and tank configuration, a  $d=36m$ ,  $h=12m$  tank was adopted in this model as tanks in under-construct Solana Generating Station in USA ( $d=37.2m$ ,  $h=10.4m$ )[6], and working Andasol Solar Power Station in Spain ( $d=36m$ ,  $h=14m$ )[7]. In terms of the power capacity ( $MW_e$ ), we adopt the most typical operating capacity of  $50 MW_e$  and future capacity.[8]

According to the melting point of HITEC ( $142^\circ C$ ) and Rankine efficient Temperature ( $\geq 400^\circ C$ ), the cold molten-salt temperature is set  $200^\circ C$  for inlet, and  $450^\circ C$  for outflow.

$f$  denotes storage factor,  $R$  denotes Rankine cycle efficiency, and  $q$  denotes  $200-450^\circ C$  equivalent heat capacity of HITEC,

$\rho_H$  the density of hot MS,  $\rho_L$  the density of cold MS. The inlet mass flow  $m$ , was calculated as follows:

$$m = \frac{P \rho_H}{q f R \rho_L} \quad (1)$$

$f=0.97$ ,  $R=0.37$ , according to its relatively small scale,  $m=405kg/s$ .

### Case settings

In this paper, we tested radial distribution in the inlet velocity, and the interplay effects of power capacity to the non-uniformity. The radial distribution of inlet velocity is achieved by fixing the total mass flow rate and changes the area percentage of central non-flow part. (**Fig 2**)Case settings are listed as follows.

Table 1: The case settings of the numerical model

Diameter of rock	Power capacity	Percentage of central non-flow area			
		0%(uniform)	20%	40%	80%
$ds=0.05$	$200 MW_e$	0%(uniform)	20%	40%	80%
	$50 MW_e$	0%(uniform)	10%	20%	40%

### Properties

A typical and with computable property molten-salt is HITEC[9]. The physical properties of it are calculated according to the curve fits to experimental measurements [10]:

$$\rho_l = 1938.0 - 0.732(T_l - 200.0) \quad (2)$$

$$\mu = \exp[-4.343 - 2.0143(\ln T_l - 5.011)] \quad (3)$$

$$k_l = -6.53 \times 10^{-4}(T_l - 260.0) + 0.421 \quad (4)$$

The specific heat of HITEC is 1561.7J/kg · K, and the effective thermal conductivity of the dual-media mixture is computed as the equations provided by Gonzo [11]. For the filler material, the density and specific heat of quartzite rock are 2201 kg/m<sup>3</sup>, and 964 J/kg · K. The porosity of the filler region is set to be 0.22 with a typical average filler particle size of 0.05 m [12].

### Governing equations

The continuity and momentum equations are as follows:

$$\frac{\partial(\varphi_l)}{\partial t} + \nabla \cdot (\rho_l \mathbf{u}) = 0 \quad (5)$$

$$\frac{\partial(\rho_l \mathbf{u})}{\partial t} + \nabla \cdot \left( \rho_l \frac{\mathbf{u}\mathbf{u}}{\varepsilon} \right) = -\varepsilon \nabla p + \nabla \cdot \tilde{\boldsymbol{\tau}} + \varphi_l \mathbf{g} + \varepsilon \left( \frac{\mu}{K} \mathbf{u} + \frac{F}{\sqrt{K}} \rho_l |\mathbf{u}| \mathbf{u} \right) \quad (6)$$

Since the HTF and the filler material may be at different temperatures due to their distinct thermal conductivities and heat capacities, the energy equation is applied separately to the two phases. For the HTF, the energy equation is:

$$\frac{\partial[\varphi_l C_{p,l}(T_l - T_c)]}{\partial t} + \nabla \cdot [\rho_l \mathbf{u} C_{p,l}(T_l - T_c)] = \nabla \cdot (k_e \nabla T_l) + h_i(T_s - T_l) \quad (7)$$

For the filler material, the energy equation is:

$$\frac{\partial[(1 - \varepsilon) \rho_s C_{p,s}(T_s - T_c)]}{\partial t} = -h_i(T_s - T_l) \quad (8)$$

## RESULTS AND DISCUSSION

Results are calculated in 2D-double precision mode within the commercial CFD software Fluent 12.0.16. The thermocline tank and boundaries are discretized into 44340 cells for the finite volume method. Spatial discretization was performed with a second-order upwind method. Transient discretization was performed with a first-order implicit formulation. The PISO algorithm is applied for pressure based solver. Non-dimensional time step  $\Delta \tau$  varies from 10<sup>-7</sup> to 10<sup>-4</sup> according to distinct periods and time independence was verified with a minimum  $\Delta \tau = 10^{-8}$  with less than 0.1% deviation. The grid independence tests are performed with 2D 112300 cells, as well as 3D intensified 163730 cells verification. And the convergence are reached with a residual less than 10<sup>-3</sup>.

In the simulation, laminar flow condition is assumed and the porous media is simulated with a source term in momentum through User Defined Functions (UDF).

## Radial distribution effects

### Thermal performance of the outflow

It has long been considered the non-uniform velocity inlet will largely undermine the thermal performance of a thermocline storage without filler materials [13]. And uniform velocity assumptions has been made to dual-media thermocline storage for a better thermocline stratification.[4] However, the calculated results are to ease the concern that the non-uniformity will largely depreciate the thermal performance of total heat output. **Fig.3** are the outflow temperature history of 200 MW<sub>e</sub> and 50 MW<sub>e</sub> output, which shows the overall close fitted curves within the different non-flow percentage and uniform condition.

**Fig.4,5** shows the specific comparison of uniform, 20%, 40% and 80% in 200 MW<sub>e</sub>. Generally, in all cases the outflow temperatures are held 450°C before thermocline layer arrives the top. When the percentage is less than 50%, with the increase of non-flow area, a tiny increase of discharge time was recorded, namely 0.8% at maximum. And the maximum of deviation can only be recorded in the beginning period of temperature falling, afterward will be about 0.4%. But when the percentage is high, like 80%, the discharge time will drop by 0.8%. (**Fig.5**)

In 50 MW<sub>e</sub> capacity, the increase of discharge time is recorded 0.4% at maximum. Different plant capacity has no significant influence on the invariability of the curves, but smaller power capacity relates milder relative deviation.

The interesting results of overall small deviations can be explained with careful first and second law analysis. For first law analysis, with a fixed mass flow rate and different inlet velocity, the inlet flow carries same heat energy but different kinetic energy. Thus the total heat output can be higher with a non-uniformed velocity. For the second law analysis, the enthalpy generation in this system mainly comes from the irreversible heat transfer and viscous resistance between rock and fluid. Though the higher percentage of non-flow lead to the greater velocity gradient and cause larger exergy loss in viscous resistance. However, the higher percentage of non-flow area equals smaller area of direct heat transfer with a 450°C-200°C temperature difference, which makes the exergy loss in heat transfer reduced. In this sense, the results are reasonable.

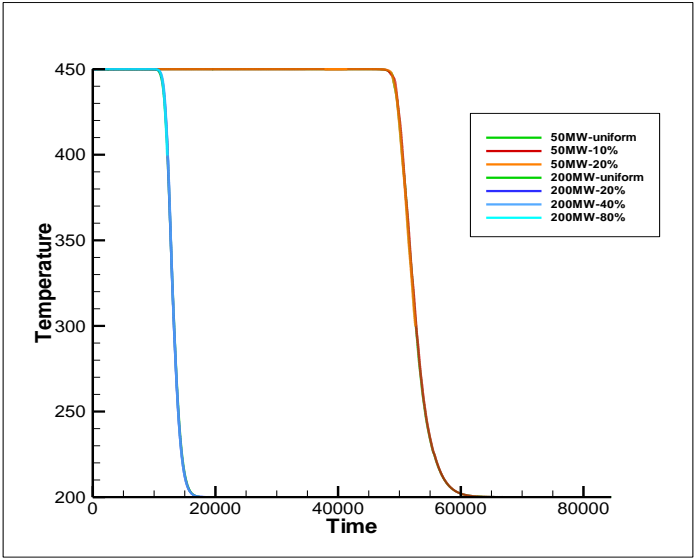


Figure 3. The temperature history (seconds) of outflow molten salt with different area of non-flow in  $50\text{ MW}_e$  and  $200\text{ MW}_e$

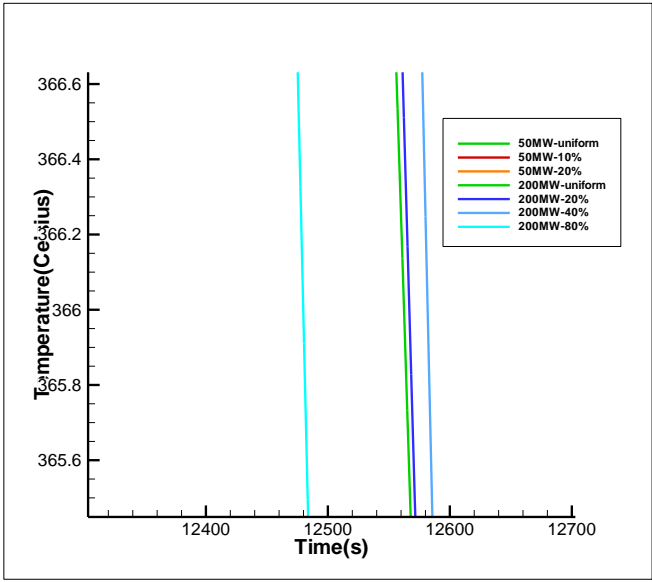
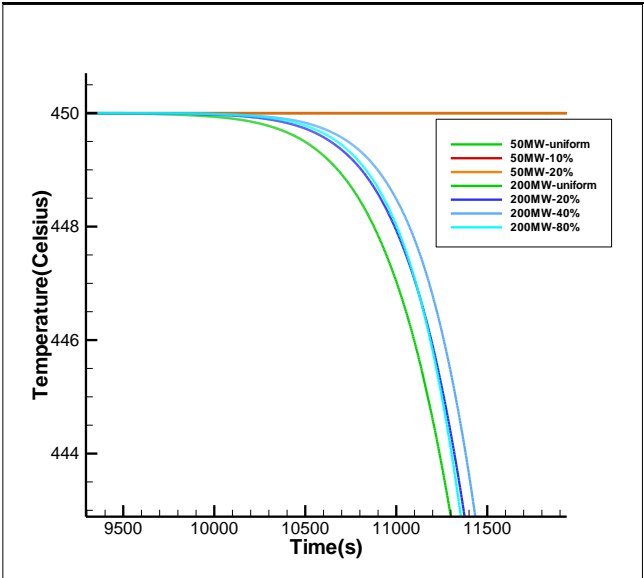


Figure 4. Specific view ( $200\text{ MW}_e$ ) the early downward period

Figure 5. Specific view ( $200\text{ MW}_e$ ) the middle downward period



**Thermocline stratification and streamline**

The different non-flow area affects the thermocline temperature distribution, mainly in the initial period of discharge. (Compare **Fig.6** with **Appendix A**). The existence of non-flow area results in the expansion of thermocline layer near the centre. Different percentage of non-flow affects the layer thickness, namely the higher percentage of non-flow, the larger span thermocline will have. Thus, the distribution non-uniformity will adversely affect the thermocline stability.

The formation of such expansion can be illustrated by the streamline of the inlet. By relating **Fig 6** and **Fig 7**, the temperature gradient are consistent with the streamline direction. The cold inlet outside the non-flow area flows towards the center (-Y direction, radial direction) as well as upward (+X direction, axial direction), thus the center area will be discharged by less cold flow and presents a higher temperature compared to the outside area within a same height X. Therefore a expansion of thermocline formed near the center. After a process of merging, the flow are eventually uniformed +X direction and form similar stratification.

Since a larger non-flow area will leave more area less discharged

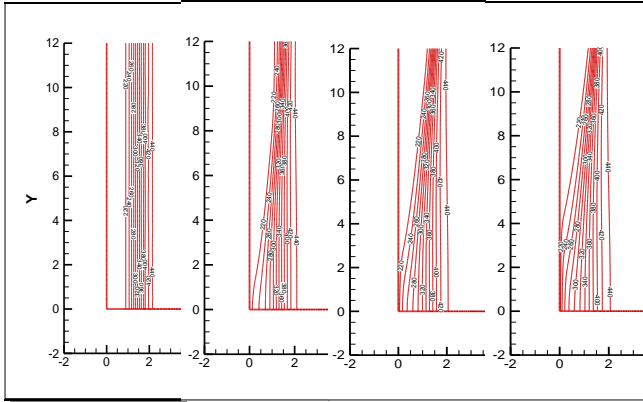


Figure 6. Thermocline temperature contours of  $200\text{ MW}_e$  after 0.1 dimensionless discharge time (left to right, uniform, 20%, 40%, 80%)

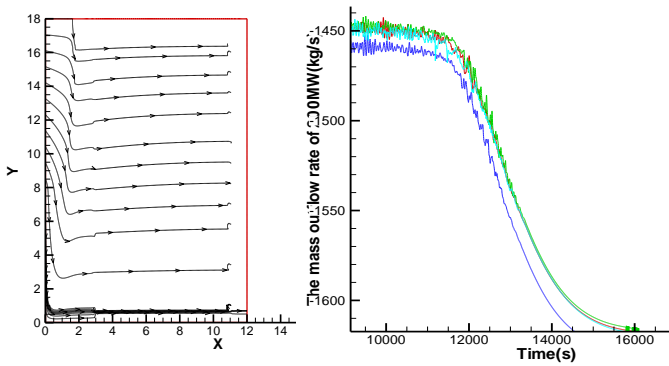


Figure 7. Inlet streamline of 20% non-flow with  $200\text{ MW}_e$   
Figure 8. Mass flow rate increase of 80% area non-flow (blue line, negative value)

### Mass flow rate

Basically, the mass flow rate multiples temperature of the outflow presents the magnitude of total heat output. And mass flow rate plays a important role in electricity generation cycle. When the percentage is low, the mass flow rate has little difference compared to the uniform condition. When 80% area is non-flow, while the temperature magnitude remains unaffected (Fig.4), the mass flow rate will increase by 0.8% (Fig.8), thus leads to a decrease of discharge time by 0.8% (mentioned in Fig.5).

The increase mass flow rate mainly result from the increased inlet velocity. And 80% percentage of radial distribution non-uniformity can be a critical indicator of maintaining constant mass flow rate.

### The synthetic effects of power capacity

Power capacity directly relates mass rate of inlet. (Eq.1)

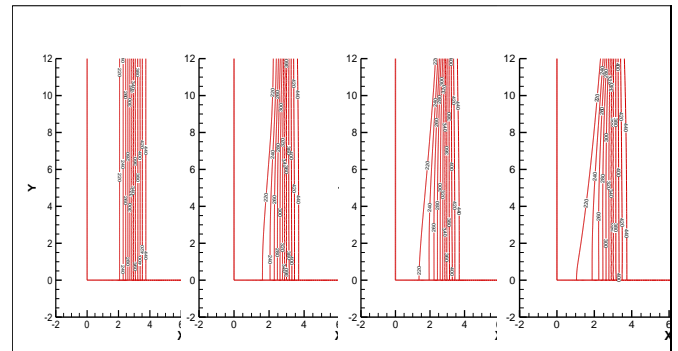
In the numerical results, smaller power capacity in settings lead to milder relative deviation and smaller expansion in thermocline stratification.

The power capacity affects the mean inlet velocity and thus the Re number and convective heat-transfer efficient, and the resistance force. Smaller Re number leads to a smaller resistance force resulting in less exergy loss in viscous resistance. However, due to the infinitesimal deviation uncertainty, further study shall be carried to give the instruction of relation between the capacity and non-uniformity effects.

### CONCLUSION

In this work, non-uniform inlet velocity condition in dual-media thermocline storage has been simulated through CFD. And the results show mild deviation in discharge time appears but no significant influence has been discovered on the thermal performance of outflow. Preliminary explanation has been made through first and second law analysis. The contours of temperature distribution in non-uniform velocity can be explained with streamline from inlet boundary. A 80% percentage of non-flow area will affect the discharge time and mass flow rate by 0.8%, further study on the relation between critical percentage and plant capacity has been recommended. Other parameters' interplay with the non-uniformity should also be studied.

### APPENDIX-A



Thermocline temperature contours of  $200\text{ MW}_e$  after 0.2 dimensionless discharge time (left to right, uniform, 20%, 40%, 80%).

We can find the difference of 3 percentages' contour is diminished with time advancing.

### REFERENCES

- [1] D. Kearney, B. Kelly, U. Herrmann *et al.*, 2004 "Engineering aspects of a molten salt heat transfer fluid in a trough solar field," *Energy*, 29( 5), pp. 861-870.
- [2] D. Brosseau, J. W. Kelton, D. Ray *et al.*, 2005 .Testing of Thermocline Filler Materials and Molten-Salt Heat Transfer Fluids for Thermal Energy Storage Systems in

- Parabolic Trough Power Plants, *Journal of solar energy engineering*, 127, pp. 109.
- [3] S. Flueckiger, Z. Yang, and S. V. Garimella, 2011, An integrated thermal and mechanical investigation of molten-salt thermocline energy storage, *Applied Energy*, 88(6), pp. 2098-2105
- [4] J. T. Van Lew, P. W. Li, C. L. Chan *et al.*, 2010, *Transient heat delivery and storage process in a thermocline heat storage system*, Amer Soc Mechanical Engineers, New York..
- [5] M. A. Karim, 2011, Experimental investigation of a stratified chilled-water thermal storage system, *Applied Thermal Engineering*, 31(11-12), pp. 1853-1860.
- [6] WebPage, *Solana Generating Station / Case Study*, The Clean Energy Action Project.
- [7] *The Construction of the Andasol Power Plants*, Solar Millennium, Spain.
- [8] WebPage, *List of solar thermal power stations*, Wikipedia.
- [9] D. Kearney, U. Herrmann, P. Nava *et al.*, "Assessment of a molten salt heat transfer fluid in a parabolic trough solar field," *TRANSACTIONS-AMERICAN SOCIETY OF MECHANICAL ENGINEERS JOURNAL OF SOLAR ENERGY ENGINEERING*, 125( 2), pp. 170-176, 2003.
- [10] Z. Yang, and S. V. Garimella, 2010, Thermal analysis of solar thermal energy storage in a molten-salt thermocline, *Solar Energy*, 84(6), pp. 974-985
- [11] E. E. Gonzo, 2002, Estimating correlations for the effective thermal conductivity of granular materials, *Chemical Engineering Journal*, vol. 90, no. 3, pp. 299-302.
- [12] Z. Yang, and S. V. Garimella, 2010, Molten-salt thermal energy storage in thermoclines under different environmental boundary conditions, *Applied Energy*, vol. 87, no. 11, pp. 3322-3329.
- [13] Phd thesis, S. Afrin, 2012, "Numerical analysis of single tank thermocline thermal storage system for concentrated solar power plant", 1518209, The University of Texas at El Paso, United States -- Texas.
- [14] J. T. Van Lew, P. W. Li, C. L. Chan *et al.*, 2010, *Transient heat delivery and storage process in a thermocline heat storage system*, Amer Soc Mechanical Engineers, New York.